

Mass sensitivity of GRACE-like geodesy missions

Robert Spero
19 June 2020

Jet Propulsion Laboratory, California Institute of Technology, Pasadena, California 91109, USA

arXiv:2006.08179v2 [physics.geo-ph] 20 Jun 2020

Corresponding author: Robert Spero, spero@jpl.nasa.gov

Abstract

The sensitivity of gravity-sensing low-low satellite-to-satellite ranging measurements in the style of GRACE is assessed as the minimum detectable point mass M_3 that gives signal-to-noise ratio = 3 as a function of orbital altitude, satellite separation, and instrument noise. We find for the laser ranging interferometer measurement on GRACE-FO $M_3 = 470$ Mton. M_3 for a range of future missions with different orbital parameters and improved instrument sensitivity is explored.

Plain Language Summary

The twin-satellite mission GRACE-FO has been measuring Earth’s changing gravity for two years, as did its predecessor GRACE for 15 years. These missions have provided information on large-scale motion of water and ice melting, information that was previously unavailable. In the next ten years more such mass-change measuring satellites will be launched to continue the gravity record with improved precision. Yet there has been no single-number answer to the question, how precisely is gravity measured by such missions? This paper derives a prescription for a sensitivity figure of merit, namely mass resolution. GRACE-FO is found to be capable in principle of measuring masses as small as 500 Mton. To set the scale, melting of Greenland ice at the rate of 300 Gton/year is easily measured by GRACE, while the weight of all the buildings in a large city is only 100 Mton. Future missions may have sensitivity on the order of 10 Mton. The mass resolution formulation developed in this paper allows an optimization of orbit and payload instruments for more precise measurements of known sources such as glaciers and changing sea level, and to discover new sources such as underground water storage that are too small to be observed by existing satellites.

1 Introduction

The GRACE (Tapley et al., 2004) and GRACE Follow-On (GRACE-FO) (Landerer et al., 2020) measurements of earth’s gravity field are based on high-precision along-track range measurements of the 200 km separation between satellites in a common near-polar low-earth orbit. The differential gravitational force on the spacecraft pair changes as it passes over inhomogeneous mass distributions, resulting in a change in the measured separation. Following Han (2013), we examine the effect of regional as opposed to global mass distributions. To construct a single-number metric for instrument-limited sensitivity, the simplest source of signal is considered: the satellite pair flying over a point mass. The minimum detectable mass M_3 is calculable as the point mass that gives signal-to-noise ratio $\rho = 3$.

2 Signal

The measurement configuration and signal parameters are shown in Figure 1.

2.1 Single Spacecraft Acceleration

Neglecting orbital dynamics, which enter at low frequency compared to the high-frequency source disturbance under consideration, the acceleration on spacecraft 1 flying over point mass M at along-track distance x is $a_1 = -GMx/(h^2 + x^2)^{3/2}$, where G is Newton’s constant of gravitation. For $M = 1$ Gton, $GM = 67 \text{ m}^3/\text{s}^2$.

Define the acceleration per unit source mass, $a'_1 = a_1/M$. Using $x = v_o t$, $v_o =$ orbital velocity, $t =$ time from $x = 0$,

$$a'_1 = -\frac{Gt v_o}{(h^2 + t^2 v_o^2)^{3/2}} \quad (1)$$

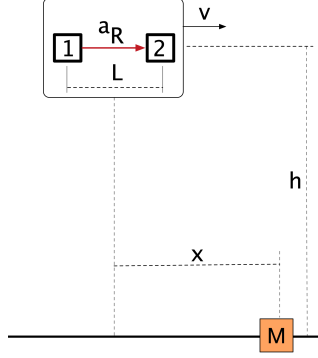


Figure 1. Parameters for differential acceleration measurement a_R between spacecraft 1 and 2 with average separation L as they fly at altitude h with common velocity v at along-track distance x from point mass M .

Convert to frequency space, acceleration as a function of f instead of t , by taking the fourier transform \mathcal{F} :

$$a'_1(f) = \mathcal{F}[a'_1(t)] = \frac{4\pi i f G K_0 \left(\frac{2\pi f h}{v_o} \right)}{v_o^2}, \quad (2)$$

where K_0 is the modified bessel function of the 2nd kind, order 0.

2.2 Range Acceleration Signal

The acceleration experienced by spacecraft 2 is the same as spacecraft 1 at distance L , but delayed by $\tau = L/v_o$. The resulting (along-track) range acceleration between the spacecraft (Figure 2, left) is similar to what Han (2013) computed for the the response of GRAIL spacecraft to regional lunar gravity. The peak range acceleration a_R^p is related to M by

$$a_R^p = \frac{GL}{(h^2 + (L/2)^2)^{3/2}} M \equiv \kappa M. \quad (3)$$

Using the identity $\mathcal{F}(\text{delay } \tau) = \exp(-2\pi i f \tau)$, the range acceleration in frequency space $a_R(f)$ is given by

$$a'_R(f) = a'_1(f)(1 - e^{-2\pi i f \tau}) \quad (4)$$

$$|a'_R(f)| = 2|a'_1(f) \sin(\pi f \tau)| \quad (5)$$

That is, in the frequency domain the range acceleration is the single-satellite acceleration multiplied by $2|\sin(\pi f \tau)|$. For $f \ll 1/\tau$, $|a_R(f)| \propto L$, which is the response for the spacecraft pair acting as a gradiometer. The first null in the response is at $f_{\text{null}} = 1/\tau = 38$ mHz for low-earth orbit and $L = 200$ km, as recognized by Wolff (1969). In degree-variance evaluations of measurement sensitivity, the first null is expressed as a maximum in geoid height error at degree $N = f_{\text{null}}/f_1 = 216$ for $L = 200$ km, and $N = 86$ for $L = 500$ km, where $f_1 = \text{orbital frequency} = 0.176$ mHz.

From Equations 2 and 5,

$$|a'_R(f)| = \frac{8\pi f G}{v_o^2} \left| K_0 \left(\frac{2\pi f}{f_h} \right) \right| \left| \sin \left(\frac{2\pi f}{f_L} \right) \right|, \quad (6)$$

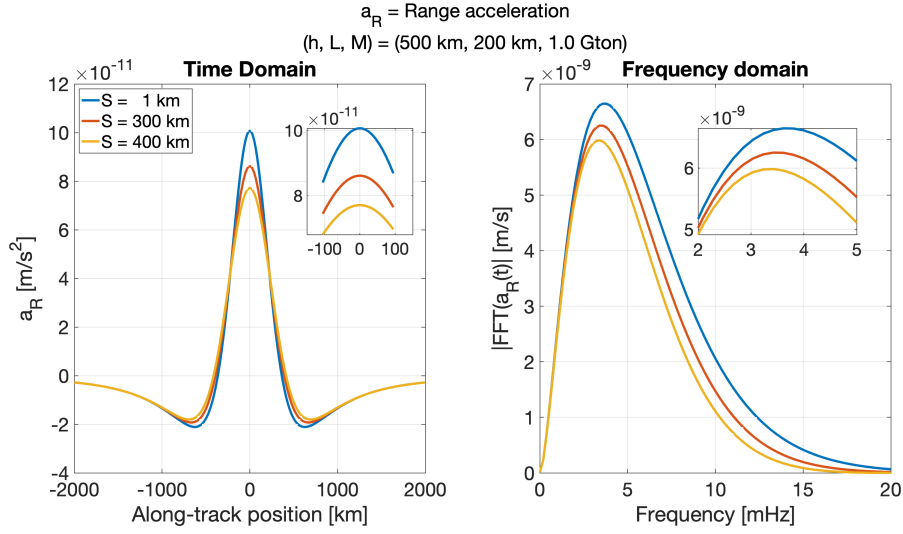


Figure 2. Range acceleration resulting from a square mass centered under the flight along-track path. Orbital altitude h , average spacecraft separation L and source mass M are indicated in the title. The separate traces are for squares of side S indicated in the legend. *Left:* time domain; *Right:* frequency domain.

where

$$\begin{aligned}
 v_o &= \text{orbital velocity} && = 7.6 \text{ km/s} \\
 h &= \text{orbital altitude} && = 500 \text{ km} \\
 L &= \text{spacecraft separation} && = 200 \text{ km} \\
 f_h &= \frac{v_o}{h} && = 15.5 \text{ mHz} \\
 f_L &= \frac{v_o}{L/2} && = 76 \text{ mHz},
 \end{aligned}$$

numerical values applicable to GRACE-FO, for which $\kappa = 0.101 \text{ nm/s}^2/\text{Gton}$.

To explore the valid span of the point-mass approximation, Figure 2 shows the range acceleration signal from a square-shaped mass of side length S , computed by numerical integration. The $S=1 \text{ km}$ result is in agreement with the point-mass analytical calculation, which is valid at the 20% level for sources as large as $S=300 \text{ km}$. Henceforth, we restrict analysis to the signal from a point source. For $f > 30 \text{ mHz}$, the signal amplitude is smaller than its peak value by more than 5 orders of magnitude.

A point disturbance gives the impulse response, and its fourier transform, Equation 6, is the transfer function from an arbitrary mass spectrum. Compared to the transfer function approach of Ghobadi-Far et al. (2018) for inferring gravity fields from range acceleration, we seek the response of the system to an artificial source, a point mass. We neglect centrifugal acceleration and spacecraft motion other than the along-track direction.

3 Noise

Under the assumption that the range measurement is limited by thermal noise of the laser reference cavity (Numata et al., 2004), the laser ranging interferometer (LRI) has displacement noise root power spectral density (rpsd) \tilde{x}_{LRI} and strain rpsd \tilde{x}_{LRI}/L

given by

$$\tilde{x}_{\text{LRI}}(f)/L = x_c/\sqrt{f}, \quad (7)$$

where x_c is a constant. For the LRI (Abich et al., 2019), $x_c = 1 \times 10^{-15}$. The rpsd of range acceleration measurement noise is

$$\sqrt{S_{\text{LRI}}(f)} = (2\pi f)^2 \cdot \tilde{x}_{\text{LRI}}(f). \quad (8)$$

Take for the accelerometer measurement noise rpsd on GRACE and GRACE-FO (Touboul et al., 1999)

$$\sqrt{S_{\text{ACC}}(f)} = \tilde{a}_0 \sqrt{1 + \left(\frac{f_k}{f}\right)^2}, \quad (9)$$

with $\tilde{a}_0 =$ acceleration white noise $= 1 \times 10^{-10} \text{ m/s}^2/\sqrt{\text{Hz}}$, $f_k = 5 \text{ mHz}$. Improved accelerometers in future missions (Christophe et al., 2010), (Conklin & Nguyen, 2017) may have $\tilde{a}_0 = 1 \times 10^{-12} \text{ m/s}^2/\sqrt{\text{Hz}}$ or better. Assuming that the accelerometers have uncorrelated noise, the total S_{ACC} is sum of the S_{ACC} from each spacecraft. We assume that the non-inertial acceleration noise is equal to the accelerometer sensing noise. This is a conservative assumption in that for part of the spectrum modeled disturbances for solar radiation pressure and thruster firings may have lower noise than the accelerometer, and, depending on orbital altitude, atmospheric drag may be smaller than accelerometer noise.

The total instrument noise power spectral density is

$$S_a = S_{\text{ACC}} + S_{\text{LRI}}. \quad (10)$$

Figure 3 shows $\sqrt{S_a}$ for various instrument noise spectra.

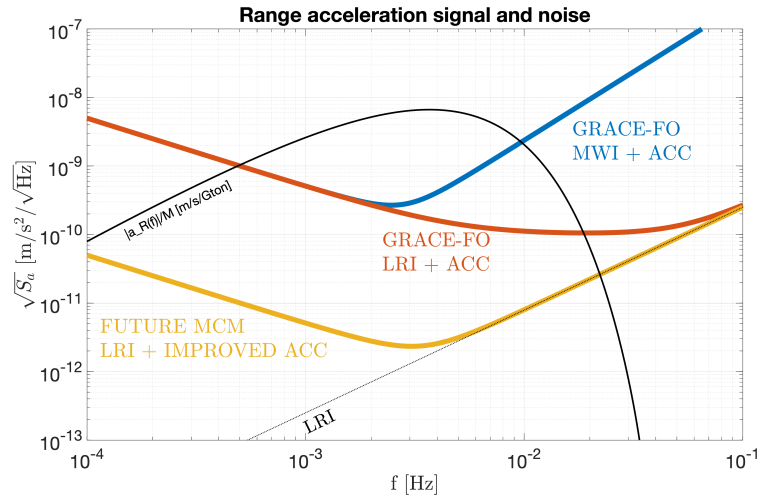


Figure 3. Total range acceleration noise rpsd $\sqrt{S_a}$ for various assumptions of instrument noise. The ranging noise for the “GRACE-FO MWI+ACC” is the white displacement noise of the microwave measurement on GRACE-FO, equal to $6 \times 10^{-7} \text{ m}/\sqrt{\text{Hz}}$. The other two noise curves assume the ranging noise of the LRI, Equation 7, shown as a dotted line. Two levels of $\tilde{a}_0/[\text{m/s}^2/\sqrt{\text{Hz}}]$ are assumed: 1×10^{-10} for the GRACE-FO curves, and 1×10^{-12} for a future mission. The solid black line is the signal spectrum $a_R(f)$ from a 1 Gton point mass, for orbital altitude $h = 500 \text{ km}$ and separation $L = 200 \text{ km}$. The values of M_3 for the three respective configurations are 1.33 Gton, 470 Mton, 9.5 Mton.

4 Detectable Mass

Following Flanagan and Hughes (1998) (see also Wainstein and Zubakov (1970)), the maximum signal-to-noise ratio ρ is given by Wiener optimal filter theory as

$$\rho = \sqrt{4 \int_0^\infty \frac{|a_R(f)|^2}{S_a(f)} df}. \quad (11)$$

The integrand of Equation 11 is shown in Figure 4 for several values of L . The oscillations with nulls at multiples of $1/\tau = v_o/L$ degrade ρ for L beyond an optimum spacecraft separation. The minimum detectable mass with $\rho = 3$ is

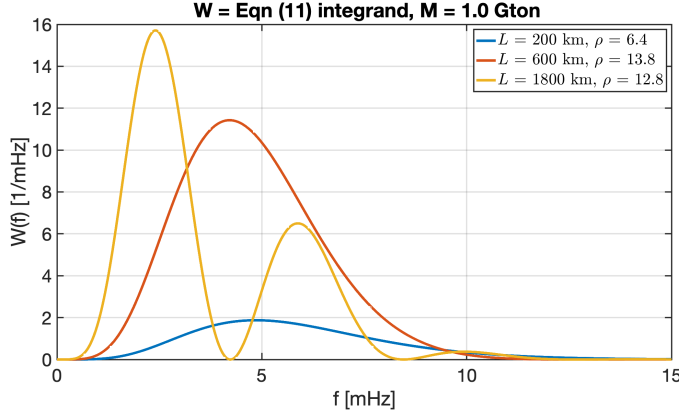


Figure 4. Integrand of Equation 11 $|a_R(f)|^2/S_a(f)$ for the “GRAE-FO LRI + ACC” noise of Figure 3, signal from orbital altitude $h = 500$ km and source mass $M = 1$ Gton and several values of spacecraft separation L . The resulting signal-to-noise ratios ρ after integration are indicated in the legend.

$$M_3 = 3/\sqrt{4 \int_0^\infty \frac{|a'_R(f)|^2}{S_a(f)} df}. \quad (12)$$

From Equations 12, 10, 9, 8, 7, 6, the GRACE-FO parameters with the MWI and LRI give respectively $M_3 = 1.33$ Gton, 470 Mton. The corresponding detectable peak acceleration for the MWI, $a_R^p = \kappa \cdot 1.33$ Gton = 0.13 nm/s², is comparable to the simulation result of Ghobadi-Far et al. (2018), who found the estimation error for the MWI to be 0.15 nm/s². A comparison point for the LRI sensitivity is inferred from Colombo and Chao (1992), who proposed a laser ranging mission that, with $(h, L) = (600, 500)$ km was found by simulation to have sensitivity to weekly changes of 1 mm water height over a region 400 km across, or mass sensitivity of 160 Mton.

Figure 5 shows the mass sensitivity as a function of h and L for the LRI ranging instrument with two levels of accelerometer sensitivity: $\tilde{a}_0 = (1 \times 10^{-10}, 1 \times 10^{-12})$ m/s²/√Hz. The optimum L for a given h depends weakly on the accelerometer noise, and is given approximately by $1.78h$ and $1.70h$ respectively. The lower row of Figure 5 shows the computed optimum L in comparison with these approximations, and the corresponding optimum M_3 .

Acknowledgments

The author thanks Christopher McCullough, Kirk McKenzie, Gabriel Ramirez, Pep Sanjuan and David Weise for useful discussions. This research was carried out at the Jet Propulsion Laboratory, California Institute of Technology, under a contract with the National

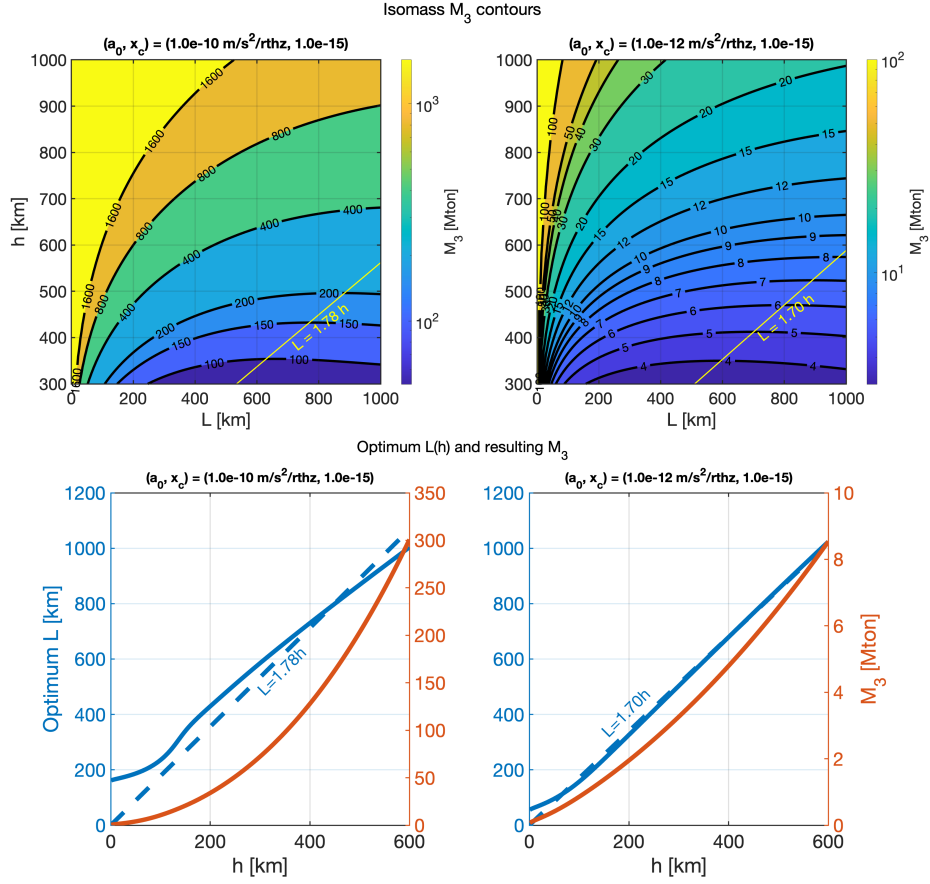


Figure 5. Mass sensitivity of of the LRI measurement on GRACE-FO *left*, and of a future GRACE-like mission *right*. Upper row shows isomass M_3 contours, in Mton, from Equation 12. Equation 7 specifies the ranging noise, and accelerometer noise is given by Equation 9 with $\tilde{a}_0 = (1 \times 10^{-10} \text{ m/s}^2/\sqrt{\text{Hz}}, 1 \times 10^{-12} \text{ m/s}^2/\sqrt{\text{Hz}})$ for the respective missions, with fixed $f_k = 5 \text{ mHz}$. The optimum satellite separation L as a function of orbital altitude h is given approximately by $L = (1.78, 1.70)h$, respectively. Lower row shows the precise optimum L as a function of h , (solid blue, left axis) and the resulting sensitivity M_3 (red, right axis).

Aeronautics and Space Administration. ©2020 California Institute of Technology. Government sponsorship acknowledged.

References

- Abich, K., Abramovici, A., Amparan, B., Baatzsch, A., Okihiro, B. B., Barr, D. C., ... others (2019). In-orbit performance of the grace follow-on laser ranging interferometer. *Physical review letters*, *123*(3), 031101.
- Christophe, B., Marque, J., & Foulon, B. (2010). In-orbit data verification of the accelerometers of the esa goce mission. In *Sf2a-2010: Proceedings of the annual meeting of the french society of astronomy and astrophysics* (Vol. 1, p. 113).
- Colombo, O., & Chao, B. (1992). Global gravitational change from space in 2001. In *Iag symposium, potsdam* (Vol. 112).
- Conklin, J., & Nguyen, A. N. (2017). Drag-free control and drag force recovery of small satellites. In *31st annual aiaa/usu conference on small satellites*.
- Flanagan, E. E., & Hughes, S. A. (1998, Apr). Measuring gravitational waves from binary black hole coalescences. i. signal to noise for inspiral, merger, and ringdown. *Phys. Rev. D*, *57*, 4535–4565. doi: 10.1103/PhysRevD.57.4535
- Ghobadi-Far, K., Han, S.-C., Weller, S., Loomis, B. D., Luthcke, S. B., Mayer-Gürr, T., & Behzadpour, S. (2018). A transfer function between line-of-sight gravity difference and grace intersatellite ranging data and an application to hydrological surface mass variation. *Journal of Geophysical Research: Solid Earth*, *123*(10), 9186–9201.
- Han, S.-C. (2013). Determination and localized analysis of intersatellite line of sight gravity difference: Results from the grail primary mission. *Journal of Geophysical Research: Planets*, *118*(11), 2323–2337.
- Landerer, F., Flechtner, F., Save, H., Webb, F., Bandikova, T., & Bertiger, e. a., WI. (2020). Extending the global mass change data record: Grace followon instrument and science data performance. *Geophysical Research Letters*, *47*. doi: 10.1029/2020GL088306
- Numata, K., Kemery, A., & Camp, J. (2004). Thermal-noise limit in the frequency stabilization of lasers with rigid cavities. *Physical Review Letters*, *93*(25), 250602.
- Tapley, B. D., Bettadpur, S., Ries, J. C., Thompson, P. F., & Watkins, M. M. (2004). Grace measurements of mass variability in the earth system. *Science*, *305*(5683), 503–505. doi: 10.1126/science.1099192
- Touboul, P., Willement, E., Foulon, B., & Josselin, V. (1999). Accelerometers for champ, grace and goce space missions: synergy and evolution. *Bollettino di Geofisica Teorica ed Applicata*, *40*(3-4), 321–327.
- Wainstein, L. A., & Zubakov, V. (1970). *Extraction of signals from noise*. Prentice-Hall, Englewood Cliffs, NJ.
- Wolff, M. (1969). Direct measurements of the earth's gravitational potential using a satellite pair. *Journal of Geophysical Research*, *74*(22), 5295–5300.